ATTENUATION AND SCATTERING STUDIES OF NATURAL AND FABRICATED PARTICLEBOARD OF *RHIZOPHORA SPP.* IN THE 15.77 – 25.27 keV PHOTON ENERGY RANGE

By

BASSAM ZUHDI OTHMAN SHAKHREET

Thesis submitted in fulfillment of the requirements for
the degree of Doctor of Philosophy

October 2006

إهداء

إلى **والدي** حفظه الله ... الذي وقف بجانبي
وعلّمني أنّ الرجال وحدهم من يقهرون الصعاب
ويصلون إلى الهدف.

إلى **والدتي** حفظها الله ... التي علّمتني أنّ المحبة
والرحمة هما سرّ الحياة السعيدة.

إلى المرأة التي كانت دائماً خلفي تدفعني نحو الإبداع ...
إلى **زوجتي** حفظها الله.

إلى **أطفالي** حفظهم الله ... الذين ضحكاتهم
تزيدني إصرارًا وقوة.

DEDICATION

This Thesis is Dedicated to My

Father

Who Has Done His Best to Uplift Me,
Without Whom I Would Not Have Been Able
To Achieve This,

To My

Mother

For Her Love and Affection,

And To My

Wife

For Her Support and Encouragement

ACKNOWLEDGEMENTS

The author's thanks and gratitude first goes to **ALLAH**, the Lord of mankind, jinn, and all that exists, who gave him the strength, inspiration and patience to continue this research. His parents are deeply indebted by him for their prayers and patience. He would like to express his gratitude to them, his wife, his sisters and his only brother who guided him along the correct path of education above their capacity. May Allah bless them, amen. I should not forget the contribution of Professor W. C. Roentgen for his wonderful discovery of x-ray, without which I would not have an opportunity to be involved in such an interesting branch of science. His thanks go also to many people who have contributed directly or indirectly in the completion of this research. Some of them deserve special mention.

The author expresses his sincere profound gratitude to his wonderful supervisor **Prof. Dr. Ahmad Shukri**, School of Physics, Universiti Sains Malaysia (USM), whose valuable instructions, cooperation, constructive criticisms and exceptional role helped bring this thesis to reality. The author is indebted to him for imparting his wide experiences and knowledge in this field.

The author is also extremely grateful to **Dr. Sabar Bauk**, his second supervisor, who guided him throughout the thesis. He provided timely feedback and affirmative suggestions. The author is very grateful to him for the extensive discussion on the relevant materials and for his suggestions on how each argument should be presented.

The fabrication of the *Rhizophora spp.* particleboard was carried out at the School of Industrial Technology (I.T.), Universiti Sains Malaysia. The author would like to thank the School of Industrial Technology for their help and in giving him the permission to use the facilities of the school. The author would like to pay tribute to **Dr. Rokiah binti Hashim**, School of Industrial Technology, USM for her support in using the school facilities and for useful discussions, suggestions, contributions, and ideas. The author is deeply indebted to **Siti Hazneza Abdul Hamid** for her great help and suggestions.

The author owes his special thanks to Malaysian Technical Cooperation Program Scholarship (**MTCP**) for providing him financial support to achieve his PhD study.

Many thanks go also to **Universiti Sains Malaysia** for giving him the chance to continue his higher education. The author would like to recognize the efforts of all the technical staffs in the Biophysics Laboratory especially **Mr. Azmi Omar** from whom he frequently needed help with many odd jobs during his research. Willing and capable staffs were always available to assist and to them he is forever grateful. The co-operation from the staff of the Dean's office, Engineering workshop, Main library and Institute of Postgraduate Studies is highly appreciated.

Finally, special gratitude and warmest thanks goes to his wonderful wife and their two daughters Ala' and Esra' for their understanding, patience and support throughout the period of his research. The author will never forget the joy and happiness that his daughters have brought to him throughout this endeavor.

Bassam Zuhdi Shakhreet

Penang, Malaysia, October 2006

TABLE OF CONTENTS

Chapter 1. INTRODUCTION

Chapter 2. CHARACTERISTICS OF DIAGNOSTIC X-RAYS

Chapter 3. PHOTON TRANSMISSION MEASUREMENTS USING X-RAY FLUORESCENT (XRF) SOURCES

Chapter 6. FABRICATING *RHIZOPHORA SPP.* PARTICLEBOARD AND MEASURING THE MASS ATTENUATION COEFFICIENT

Chapter 7. SUMMARY AND CONCLUSION

APPENDICES

LIST OF TABLES

LIST OF FIGURES

LIST OF APPENDICES

LIST OF SYMBOLS AND ABBREVIATIONS

A	Atomic weight.
AD wood	Air dried wood.
Ag	Silver.
Al	Aluminum.
c_n	The number of counts in the n^{th}.
c_{n+1}	The number of counts in the n^{th} +1.
CST	Compton Scattering Tomography.
$\frac{d\sigma_R}{d\Omega}$	Rayleigh differential scattering cross section.
$\frac{d\sigma_{TH}}{d\Omega}$	Thomson differential scattering cross section.
ε_a	The absolute efficiency.
ε_i	The intrinsic efficiency.
δE	The full-width at half-maximum measured in the number of channels.
f	Fractional change.
f_i	Fractional weight of the ith element of the mixture.
$F(q)$	Atomic form factor.
FOV	Field of view.
FWHM	Full Width at Half Maximum
FWTM	Full Width at Third Maximum.
h	Plank constant.
I	Intensity of attenuated XRF beam.
I_o	Initial intensity of XRF beam.
l_c	Length of collimator.
In	Indium.
LFF	Long Fine Focus.
L_{opt}	Optimum sample thickness.
m_o	Rest mass of electron.
mc	Moisture content.
MCA	Multichannel analyzer.
MF	Melamine formaldehyde.
m_{n+1}	Mass of added element.
Mo	Molybdenum.

MUF	Melamine-urea formaldehyde.
N_A	Avogadro's number (6.0223×10^{23} mole^{-1}).
N_e	Electron density (number of electron per gram).
N_o	Initial number of photons in the beam.
n	Number of atoms per unit volume of the target.
NH_3	Ammonia.
NH_4Cl	Ammonium chloride.
OD	Optical density.
OD wood	Oven dried wood.
ρ	Physical density (gm cm^{-3}).
Pd	Palladium.
$P(E_\gamma,\theta)$	Ratio of photon energy before and after the collision.
ρ_e	Electron density (number of electron per unit volume).
PF	Phenol formaldehyde.
PH	Hydrogen ion concentration.
p_i	Fractional abundance by weight of the ith constituent element.
p_i'	New fractional abundance of the ith constituent element.
p_{n+1}	Proportion by weight of the added element.
r	Radius.
R	Resolution.
r_e	Classical electron radius (2.8179×10^{-15} m).
Sn	Tin.
T_{e+}	Kinetic energy of the positron.
T_{e^-}	Kinetic energy of the ejected electron.
μ	Linear attenuation coefficient (m^{-1}).
μ/ρ	Mass attenuation coefficient (cm^2 gm^{-1}).
$(\mu/\rho)_i$	Corresponding mass attenuation coefficient.
UF	Urea formaldehyde.
XCOM	Computer code.
χ^2	Chi square.
Z	Atomic number.
Zr	Zirconium.
$(\bar{Z})$	The effective atomic number of mixture.
Ω	The solid angle.

KAJIAN PENGECILAN DAN SERAKAN BAGI *RHIZOPHORA SPP* TABII DAN PAPAN HABUK TERFABRIKASI DALAM JULAT TENAGA FOTON 15.77 – 25.27 KEV

ABSTRAK

Pekali pengecilan jisim bagi Rhizophora *spp.* ditentukan dalam julat tenaga 15.77 - 25.27 keV menggunakan kaedah berasaskan pendarfluoran sinar-X (XRF) dilengkapi satu aturan sistem dengan geometri bentuk-L dan satu pengesan Si-PIN.

Prestasi setiap komponen dalam aturan tersebut diuji secara berasingan dan ciri masing-masing direkod untuk kegunaan optimum. Sistem XRF tersebut seterusnya diteliti sebagai satu himpunan sepadu.

Untuk memperolehi maklumat ketumpatan elektron sebagai penyokong kepada penggunaan bahan setara tisu yang baru untuk fantom mamografi, ketumpatan elektron kayu *Rhizophora spp.* diukur dan ditentukan. Nilai yang diukur pada tenaga 15.77, 17.48 dan 22.16 keV, iaitu (3.183 ± 0.003) x 10^{23} e/cm^3 didapati amat hampir dengan nilai yang dihitung iaitu (3.195 x 10^{23} e/cm^3). Tambahan pula, kejituan nilai tersebut amat baik. Pada amnya nilai ketumpatan elektron untuk air (3.341 x 10^{23} e/cm^3) dan ketumpatan elektron untuk payudara dalam julat (3.120 – 3.510) x 10^{23} e/cm^3 (ICRU, 1992) boleh dianggap sesuai untuk perbandingan dengan nilai untuk *Rhizophora spp.*

Pekali pengecilan jisim bagi *Rhizophora spp.* tabii daripada tiga bahagian berbeza dari batang sesuatu pokok (bahagian atas, tengah dan bawah) ditentukan dalam julat tenaga foton 15.77 hingga 25.27 keV. Ini dilaksanakan

dengan mengukur pengecilan foton XRF daripada sasaran zirkonium (Zr), molibdenum (Mo), paladium (Pd), perak (Ag), indium (In) dan timah (Sn). Kedua-dua puncak K_α dan K_β digunakan. Hasil yang diperolehi dibandingkan dengan nilai teori untuk tisu payudara untuk kumpulen umur muda, umur sederhana dan umur tua yang dihitung menggunakan kod komputer XCOM, kod yang dikenali dalam bidang saling tindakan sinaran untuk perhitungan pekali pengecilan dan keratan rentas saling tindakan.

Pekali pengecilan jisim yang diukur bagi bahagian tengah pokok untuk tenaga alur pendarfluoran sinar-X berlainan dalam julat tenaga berkaitan didapati memang hampir dengan nilai yang dihitung oleh XCOM untuk payudara dengan umur muda. Daripada data tersebut, didapati bahawa orientasi ira kayu tidak mempengaruhi secara signifikan ciri-ciri pengecilan jisim bagi sampel dari bahagian pokok yang sama. Pekali pengecilan jisim yang diukur dari bahagian tengah batang pokok dari lima puluh batang pokok yang berbeza didapati amat hampir dengan nilai yang dihitung untuk payudara umur muda.

Pekali pengecilan linear dan pekali pengecilan jisim bagi fantom *Rhizophora spp* papan habuk juga ditentukan dalam julat tenaga yang sama dan hasil pengukuran dibandingkan menggunakan XCOM. Pekali pengecilan jisim sampel yang dikaji didapati menghampiri nilai yang dihitung oleh XCOM untuk payudara umur tua. Pada amnya didapati bahawa pekali pengecilan jisim papan habuk *Rhizophora spp.* untuk semua ketumpaton sampel amat hampir dengan pekali yang dihitung oleh XCOM untuk payudara umur tua sementara korelasi paling kuat ialah untuk papan dengan ketumpatan 1.00 g/cm^3.

ATTENUATION AND SCATTERING STUDIES OF NATURAL AND FABRICATED PARTICLEBOARD OF *RHIZOPHORA SPP* IN THE 15.77 – 25.27 KEV PHOTON ENERGY RANGE

ABSTRACT

Mass attenuation coefficients of *Rhizophora spp.* were determined in the photon energy range of 15.77 - 25.27 keV using a method based on X-ray fluorescence (XRF) with a system setup in L-shape geometry and utilizing a Si-PIN detector.

The performance of each individual component in the setup was tested separately and its characteristics recorded for optimal use. The XRF system was then examined as an integrated assembly.

To provide electron density information in support of the introduction of new tissue equivalent materials for mammography phantoms, the electron density of *Rhizophora spp.* wood was also measured and determined. The measured value $(3.183 \pm 0.003) \times 10^{23}$ e/cm^3 at photon energies 15.77, 17.48 and 22.16 keV is reasonably close to the calculated value of $(3.195 \times 10^{23}$ e/cm$^3)$. Furthermore, the accuracy of the values is good. In general, the electron density of water $(3.341 \times 10^{23}$ e/cm$^3)$ and the electron density of values for breast tissues ranging from $(3.120 - 3.510) \times 10^{23}$ e/cm^3 (ICRU, 1992) are comparable to the measured *Rhizophora spp.* values.

The linear and the mass attenuation coefficients of natural *Rhizophora spp.* phantom from three different parts of one tree (top, middle, and bottom) were determined in the photon energy range of 15.77 to 25.27 keV. This was

performed by measuring the attenuation of XRF photons from zirconium (Zr), molybdenum (Mo), palladium (Pd), silver (Ag), indium (In) and tin (Sn) targets. Both K_α and K_β peaks were utilized. The results were compared with theoretical values for average breast tissues for young-age, middle-age, and old-age groups calculated by using XCOM computer code, the well-known code for calculating attenuation coefficients and interaction cross sections.

The measured mass attenuation coefficients of the middle part of the tree for the different X-ray fluorescent beam energies were found to be very close to the calculated XCOM values for young-age breast in this photon energy ranges. From the data it was found that the orientation of the wood grains did not significantly affect the measured mass attenuation properties of the sample from the same part of the tree.

It was also found that the measured mass attenuation coefficients of fifty different trees from the middle part were very close to the calculated value for young age breasts.

The mass attenuation coefficients of the *Rhizophora spp.* particleboard phantoms were also determined in the same photon energy range. The results were compared with theoretical values for average breast tissue for young-age, middle-age, and old-age groups calculated by using XCOM. It was found that the mass attenuation coefficient of samples tended to be close to the calculated XCOM values for old-age breasts. It is seen also that the mass attenuation coefficient of particleboards of *Rhizophora spp.* for all sample densities are very close to the XCOM calculated mass attenuation coefficient of old age breasts while the strongest correlation of them is the board which has density of 1.00 g/cm^3.

CHAPTER 1

INTRODUCTION

1.1 Introduction

Mammography is a special type of X-ray imaging that uses low energy X-rays; high contrast, high-resolution film; and an X-ray system designed specifically for mammography to create detailed images of the breast. It is used to detect and diagnose breast disease in women who either have breast problems such as a lump, pain, or nipple discharge, as well as a screening mechanism for women who have no breast complaints. Successful treatment of breast cancer depends on early diagnosis. Mammography plays a major role in the early detection of breast cancers. Mammography cannot prove that an abnormal area is cancer, but if it raises a significant suspicion of cancer, tissue will be removed for a biopsy.

Mammography has been used for about 30 years, and in the past 15 years technical advancements have greatly improved both the technique and results. Today, dedicated equipment, used only for breast X-rays, produces studies that are high in quality but low in radiation dose. Radiation risks are considered to be negligible. A mammogram is like a fingerprint; the appearance of the breast on a mammogram varies tremendously from woman to woman, and no two mammograms are alike.

It is seldom possible to measure dose distributions directly in-patients treated with radiation. So, when measuring the dose delivered to a patient, the latter is often substituted by a phantom of the same general size and shape as the relevant part of the body and made of tissue-equivalent material. This is a material, which matches tissue as regards density and effective atomic number. It therefore absorbs and scatters an X-ray beam, whatever its energy, in the same manner and to the same extent as the same volume of tissue. These conditions are most easily met by water in a thin-walled plastic container. Alternatively, specially compounded rubber, wax or wood may be used.

Basic dose distribution data are usually measured in a water phantom, which closely approximates the radiation absorption and scattering properties of muscle and other soft tissues. Another reason for the choice of water as a phantom material is that it is a universally available with reproducible radiation properties. A water phantom, however, poses some practical problems when used in conjunction with ionization chambers and other detectors, which are affected by water, unless they are designed to be waterproof. In most cases, the detector is encased in a thin plastic (water equivalent) sleeve before immersion into the water phantom.

Since it is not always possible to put radiation detectors in water, solid dry phantoms have been developed as substitutes for water. Ideally, for a given material to be tissue or water equivalent, it must have the same effective atomic number, number of electrons per gram, and mass density.

Attix (1986) defined the phantom material as a mass of solid or liquid medium that is designed to simulate the attenuation properties of the human body. White and Constantinou (1982) defined the term tissue equivalent material as that which has mass interaction data over a given energy interval and a mass density within 1 % of similar data for a tissue. They have summarized the history of using and developing the tissue substitute material and the extract below is taken from their publication:

> "All tissue substitutes appear to stem from water, suggested by Kienbock (1906) as a muscle substitute in 1906. Seven years later, the first solid (bakelite) was used and during the next 50 years, basic materials such as wax, pressed wood, glass, aluminum, and many polymers were employed in a diversity of experimental arrangements. The intensive use of both water and wax in dosimetric studies from the mid 1920s to the late 1930s had indicated the low photon attenuation properties of pure wax when compared to water and muscle".

Earlier theoretical evaluations of plastic phantoms with high energy X-rays applying scaling factors have shown to be comparable with water (Peschel and Schulz, 1974). Schulz and Nath (1979) investigated polystyrene and plastic phantoms using cesium-137 (^{137}Cs) and iodine-125 (^{125}I) gamma rays, finding the constant atomic compositions and electron densities to be suitable for their use as phantoms for high-energy X-rays and electrons.

There have been many artificial and natural materials, which have been studied and categorized as water equivalent materials. The behavior of radiation in these materials was studied in order to determine their radiological properties. Many types of wood have also been studied before such as mangrove wood; *Rhizophora spp.*, to determine their equivalence to water (Bradley *et al.*, 1991).

The term 'mangrove', is used in the broad sense either to refer to the highly adapted plants found in tropical intertidal forest communities or the ecosystem itself. The term 'mangrove' may have been derived from a combination of the

Malay word *'manggi-manggi'*, for a type of mangrove tree *Avicennia* and the Arabic *'el gurm'*, for the same, as *'mang-gurm'*.

Rhizophora spp. can be found growing profusely in the tropical muddy tidal plain in the coastal areas of the world. At the moment they are mainly used as a firewood, charcoal, construction material such as scaffolding and pilling, and also used for building small jetties. Its suitability as tissue- equivalent material was further studied by many investigators to include photon scattering.

In this study, the mass attenuation coefficients of *Rhizophora spp.* were determined in the photon energy range of 15.77 – 25.27 keV. This was done by studying the attenuation of X-ray fluorescent (XRF) photons from zirconium, molybdenum, palladium, silver, indium and tin targets. Both the K_α and K_β peaks were utilized. The results were compared with theoretical values for average breast tissues for young-age, middle-age and old-age groups calculated by using XCOM computer code (Berger and Hubbell 1987) based on the elemental composition suggested by Constantinou (1982).

XCOM is a computer program and data base which can be used to calculate photons cross sections for scattering, photoelectric absorption and pair production, as well as total attenuation coefficients, in any element, compound, or mixture, at energies from 1 keV to 100 GeV. The program is available at the National Institute of Standards and Technology (NIST) web site (http://www.physics.nist.gov/PhysRefData/Xcom/Text/XCOM.html). The XCOM program can generate cross sections on a standard energy grid (spaced approximately logarithmically), or on a grid selected by the user, or for a mix of both grids. Cross sections at energies immediately above and below all absorption edges are automatically included. XCOM provides two forms of output: (a) tables which correspond closely in format to existing tables in the literature; (b) graphical display of the tabular data.

1.2 Literature Review

Breast cancer is a major health problem as it is the most common cancer in women (Zapka *et al.* 1992). Mammographic techniques used for breast cancer screening programs need to be of the highest quality; hence, the need of good phantom materials to mimic breast tissues for use in mammographic quality assurance protocols.

There is a great necessity to find suitable materials to be used as tissue equivalent material. Many efforts have been done to evaluate the ability of a wide range of materials to be used in dose calibration.

Water is the primary phantom medium recommended for dosimetry of high-energy photon and electron beams. Its measurements closely approximate the values of radiation absorption and scattering obtained for muscle and other soft tissue. Since it is not always practical to perform dosimetric measurements in a water phantom, solid homogeneous phantoms such as polystyrene, acrylic and phantoms made from proprietary materials have found considerable popularity, particularly for clinical dosimetry (Khan, 1992).

The attenuation coefficients of various elements and compounds of dosimetric interest have been tabulated by a number of workers (Hubbell, 1982: Berger and Seltzer, 1983). However, many of the so-called tissue equivalent materials fail to provide good simulation to water at both low and high energies. White (1977) has formulated tissue substitutes for a wide range of applications (for example dosimetric phantoms, radiographic test objects and dosimeter components), the material composition being derived for both photon and electron interactions.

Attenuation studies on *Rhizophora spp.* have been found to provide close agreement with attenuation results for water for certain photon energies. Che Wan Sudin *et al.* (1988) examined the linear and mass attenuation coefficients of a number of media including a range of tropical hardwoods using a point americium-241 (^{241}Am) source at photon energy of 59.54 keV. The preliminary results indicated that the species *Rhizophora spp.* has attributes that would seem to make it a particularly good muscle or water equivalent media for dosimetric purposes.

In the present study the suitability of two materials, *Rhizophora spp.* wood and particleboard (chips-compressed) of the *Rhizophora spp.* wood for use in dose calibration in the mammographic energy range are investigated.

Rhizophora spp. wood is considered a strong wood and is suitable for structural applications. This wood is hard and heavy. There are however some disadvantages of using the raw material of *Rhizophora spp.* in radiation dosimetry studies especially with regards to phantom design.

The disadvantages are:

a) The trunk diameter of *Rhizophora spp.* trees is limited where the maximum diameter which is available in around 28 cm.
b) It is a hardwood and heavy to handle, so it is difficult to cut and shape it.
c) With long periods of time, the *Rhizophora spp.* chunks are observed to be cracked through the drying process.
d) Similarly, with long periods of time, the slabs of *Rhizophora spp.* tend to be curved or arched which causes unsymmetrical deformations in the slabs which may cause problems in stacking of slabs.

To account for the above disadvantages of raw (natural) *Rhizophora spp.*, another way to modify this natural wood to be flexible for use as a phantom for radiation dosimetry has to be found. It is for this reason that the focus in this work has been on fabricating particleboards of *Rhizophora spp.*

The benefits of the particleboard use in the radiation dosimetry work are:

a) The fact that their properties can be engineered with unlimited size.

b) Ease of cutting and shaping fabrication.

c) No obvious deformation over long periods of time.

d) Homogeneous slabs can be obtained.

e) Ease of modification by adding some materials or adhesives.

Bradley *et al.* (1991) has studied and determined the linear attenuation coefficient properties of a range of tropical hardwoods at the americium-241 photon energy of 59.54 keV. They found that *Rhizophora spp.* has the potential to become a tissue-equivalent phantom material for radiation dosimetry as its characteristics were similar to water in terms of mass-density and also attenuation. At cobalt-60 (^{60}Co) energies seasoned *Rhizophora spp.* with mass-density of 1040 kg/m^3 provided a percentage depth-dose that provided agreement to within 2 % with the tabulated values of water. Che Wan Sudin (1993) has studied the composition of *Rhizophora spp.*, finding it favorably comparable with water.

Further investigations of this wood by Tajuddin *et al.* (1996) included examining the transmission and scattering intensity for a range of hard woods, water, and modified rubber for eight scattering angles covering the range 10° – 45°. Samples of *Rhizophora spp.* and modified rubber submerged in water were radiographed and their film optical densities compared with water. The results

To account for the above disadvantages of raw (natural) *Rhizophora spp.*, another way to modify this natural wood to be flexible for use as a phantom for radiation dosimetry has to be found. It is for this reason that the focus in this work has been on fabricating particleboards of *Rhizophora spp.*

The benefits of the particleboard use in the radiation dosimetry work are:

a) The fact that their properties can be engineered with unlimited size.

b) Ease of cutting and shaping fabrication.

c) No obvious deformation over long periods of time.

d) Homogeneous slabs can be obtained.

e) Ease of modification by adding some materials or adhesives.

Bradley *et al.* (1991) has studied and determined the linear attenuation coefficient properties of a range of tropical hardwoods at the americium-241 photon energy of 59.54 keV. They found that *Rhizophora spp.* has the potential to become a tissue-equivalent phantom material for radiation dosimetry as its characteristics were similar to water in terms of mass-density and also attenuation. At cobalt-60 (^{60}Co) energies seasoned *Rhizophora spp.* with mass-density of 1040 kg/m^3 provided a percentage depth-dose that provided agreement to within 2 % with the tabulated values of water. Che Wan Sudin (1993) has studied the composition of *Rhizophora spp.*, finding it favorably comparable with water.

Further investigations of this wood by Tajuddin *et al.* (1996) included examining the transmission and scattering intensity for a range of hard woods, water, and modified rubber for eight scattering angles covering the range 10° – 45°. Samples of *Rhizophora spp.* and modified rubber submerged in water were radiographed and their film optical densities compared with water. The results showed that *Rhizophora spp.* and modified rubber have similar scattering and radiographic properties to that of water. Abdel_Munem (1999) measured the radiation dose rate distributions around brachytherapy sources, showing for dose distributions around ^{137}Cs and irredium-192 (^{192}Ir) sources in *Rhizophora spp.* wood phantom and water phantom using thermoluminescent dosimeters (TLD), that there is general agreement between results for *Rhizophora spp.* and water. Banjade *et al.* (2001) have measured the percentage depth-dose for photons at 6 MV and 5 and 12 MeV electron beams. They found that for 6 MV photon and 5 MeV electron beams, discrepancies between percentage depth-dose for *Rhizophora spp.* and water, at all depths, is found to be within 2.6% and 2.4% respectively. At 12 MeV electron energies, the measured percentage depth-dose in *Rhizophora spp.* beyond 3.5 cm depth is found to be in significant discord with those for water. Bauk *et al.* (2000) have investigated the dose distribution in *Rhizophora spp.* in an effort to determine its usefulness as an alternative phantom material for brachytherapy procedures.

Note should perhaps also be made of the efforts of a number of other workers in attempts towards characterizing photon attenuation for wood. Woods *et al.* (1965) have investigated the effect of moisture content upon mass-attenuation coefficients and half-value thicknesses at photon-energies of a few-hundred keV. Their results on Loblolly pinewood showed this wood to have mass-attenuation coefficients very similar to that for water while half-value thickness (changing linearly with change in linear attenuation coefficients) depends significantly upon moisture content. Olson and Arganbright (1981) predicted values of mass-attenuation coefficients by weighting tabulated elemental mass-attenuation coefficients by the respective elemental weight fractions. Sensitivity towards photon-energy, demonstrable below 40 keV, is not observed at higher photon energies.

From an extensive literature review no information was found about any significance differences in mass attenuation coefficient of wood samples taken from different parts of a tree or different trees. The effect of the orientation of the wood grains on the measured mass attenuation properties was also never studied. In the present work, a thorough investigation is carried out with regards to all the above issues namely variations within samples from different parts of a tree and effects of the orientation of wood grain. *Rhizophora spp.* is then evaluated as a water equivalent phantom medium for mammographic low energy photons in terms of mass attenuation coefficients and electron density.

1.3 Objectives and Scope

The main objective of the work is to carry out a thorough investigation of the radiation characteristics of *Rhizophora spp.* wood in the mammographic energy range which have never been attempted before. Previous work has focused mainly on photons at therapeutic energies. The scope of work here involves measurements of natural *Rhizophora spp.* and chips-compressed *Rhizophora spp.* for the photon-energy range between 15.77 to 25.27 keV. The use of chips-compressed *Rhizophora spp.* (as no body had worked with it before) in this study for some disadvantages of natural *Rhizophora spp.* which are mentioned in section 6.8.

The specific objectives of the present study reported in this thesis are:

1) To set up the photon source, the photon detector system and the supporting electronic units which is considered the first phase to be undertaken in the

project. This phase involves the individual testing of the equipments in an L-shape set up.

2) To identify and fabricate collimators, collimator stands and shielding; and to choose the most suitable XRF energy and hence the most suitable targets.
3) To study the parameters that affects the performance of the system in order to optimize the best working condition of the system.
4) To determine the electron density of natural *Rhizophora spp.*
5) To measure the linear and mass attenuation coefficients of natural *Rhizophora spp.* wood of the same and different trees for a range of selected XRF energies in the mammographic energy range.
6) To study the accuracy and precision of data due to samples from different parts of the same trees, samples from different trees and curing effects.
7) To fabricate *Rhizophora spp.* particleboards which can provide radiation characterization similar to natural *Rhizophora spp.* in the mammographic energy range.
8) To measure the linear and mass attenuation coefficients of particleboard (chips-compressed) *Rhizophora spp.* wood for a range of selected XRF energies in the mammographic energy range.

1.4 Outline of the thesis

This work is an attempt to determine the photon attenuation properties and electron density of *Rhizophora spp.* for the photon energy range below 60 keV. This energy region falls in the conventional mammographic X-ray energy range. The thesis is divided into seven chapters with Chapter 1 being the introduction. After a brief discussion of the theoretical aspects of diagnostic X-rays in

Chapter 2, the determination of the most suitable parameters and X-ray fluorescence system geometry are discussed in Chapter 3, which provide guidelines in selecting the effective experimental parameters used in this work.

The characterization of *Rhizophora spp.* as breast tissue equivalent is discussed in Chapter 4. The investigation mainly includes the study on the electron density of the natural *Rhizophora spp.*

Chapter 5 discusses the investigation of natural *Rhizophora spp.* phantom by measuring the mass attenuation coefficient of the sample from the same tree and from different trees. The new phantom is expected to be a potential candidate for mammography dosimetry.

Finally, Chapter 6 describes and discusses a new fabricated breast phantom. Because there are some disadvantages of using the raw material of *Rhizophora spp.* in radiation dosimetry studies, the thesis investigates the new modified phantom of the same type of wood for use as a phantom for radiation dosimetry.

Chapter 7 concludes the findings and proposes a number of suggestions for future work.

CHAPTER 2

CHARACTERISTICS OF DIAGNOSTIC X-RAYS

2.1 Introduction

X-ray photons are part of the electromagnetic family that includes light of all types (infrared, visible, and ultraviolet), radio waves, radar and television signals, and gamma rays. In a modern X-ray tube the number of electrons accelerated towards the anode depends on the temperature of the filament, and the maximum energy of the X-ray photons produced is determined by the accelerating voltage – kilovolt peak (kV_p). An X-ray tube operating at 80 kV_p will produce X-rays with a spectrum of energies up to a maximum of 80 keV.

The kilovolt peak used for an X-ray study depends on the thickness of the patient and the type of study being done. X-ray studies of the breast (mammography) are usually done at 25 to 50 kV_p, while some hospitals use up to 350 kV_p for chest X-rays.

The intensity of the X-ray beam produced when the electrons strike the anode is highly dependent on the anode material. In general, the higher the atomic number (Z) of the target, the more efficiently X-rays are produced. The target material used should also have a high melting point since the heat produced when the electrons are stopped in the surface of the target is substantial. Nearly all X-ray tubes use tungsten targets. The atomic number (Z) of tungsten is 74, and its melting point is about 3400 °C.

The electron current that strikes the target is typically 100 to 500 mA – some units even have currents of over 1000 mA. The power at the target of an X-ray tube with a current of 1 Ampere operating at 100 kV is 1×10^5 W or 100 kW, and over 99 % of this power appears as heat. The ratio of the energy that goes into X-ray photons to the energy that goes into heat is approximately $10^{-9}\ ZV$, where Z is the atomic number of the target.

2.2 Interaction of X-rays with matter

An X-ray photon can interact with the medium it is traversing by many processes. In general, X-ray photons can be either absorbed or scattered. A collimated beam of X-ray photons has an exponential attenuation nature, since each X-ray photon is absorbed or scattered in one single event which means that any photon, in the incident beam, which passes the material had no interaction what so ever. The absorption law can be written as follows:

$$I = I_o\, e^{-\mu x} \qquad (2.1)$$

where I_o is the initial intensity, I intensity after passing a medium of thickness x, and μ is the linear attenuation coefficient. The linear attenuation coefficient is dependent on the energy of the X-ray photons; as the beam becomes harder, it decreases.

The possible processes of X-ray photon interactions can be deducted from the classification done by Fano (1953), which depends on both the type and effect of the interactions as seen in Table 2.1. There are twelve combinations between the two columns representing the possible interaction processes that can be obtained. Some processes dominate over others depending on the energy range.

Table 2.1 *Type and effect of possible interaction processes.*

Type of interaction	Effect of interaction
1) interaction with atomic electrons	a) complete absorption
2) interaction with nucleons	b) elastic (coherent) scattering
3) interaction with electric field surrounding nuclei or electrons	c) inelastic (incoherent) scattering
4) interaction with meson field surrounding nucleons	

The processes of interest can be listed as follows:

(i) Photoelectric effect (1a)

(ii) Compton scattering (1c)

(iii) Pair production (3a)

(iv) Rayleigh Scattering (1b)

(v) Nuclear Thomson scattering (2b)

(vi) Delbruck scattering (3b)

(vii) Nuclear resonance scattering (2c)

(viii) Photo disintegration of nuclei (2a)

(ix) Meson production (4a)

In the energy range from a few keV up to a few MeV, the most common processes are the first three processes listed above in addition to the Rayleigh scattering process. A brief description of these four processes, which are considered to be useful, is given in the following subsections.

2.2.1 Photoelectric effect

This process occurs in the energy range 1 – 100 keV, and it involves the removal of bound electrons from the atoms upon the absorption of all the incident photon energy. The energy of the photon, E should be equal to or larger than the electron binding energy, BE. For the latter case, an electron will be ejected with kinetic energy, T given by:

$$T = E - BE \tag{2.2}$$

The electron is ejected from the atom by the incident photon energy and begins to pass through the surrounding matter. The electron rapidly loses energy and moves only a relatively short distance from its origin.

The photon energy is, therefore, deposited in the matter close to the site of the photoelectric interaction. The energy transfer is a two step process. The photoelectric interaction in which the photon transfers its energy to the electron is the first step. The depositing of the energy in the surrounding matter by the electron is the second step.

Photoelectric interactions usually occur with electrons that are firmly bound to the atom, that is, those with a relatively high binding energy but slightly less than the energy of the photon. If the binding energy is more than the energy of photon, a photoelectric interaction cannot occur. This interaction is possible only when the photon has sufficient energy to overcome the binding energy and remove the electron from the atom.

The photon's energy is divided into two parts by the interaction. A portion of the energy is used to overcome the electron's binding energy and to remove it from the atom. The remaining energy is transferred to the electron as kinetic energy and is deposited near the interaction site. Since the interaction creates a vacancy in one of the electron shells, typically the K or L, an electron moves down to fill in. The drop in energy of the filling electron often produces a characteristic radiation depends on the binding energy of the electrons involved.

Characteristic radiation initiated by an incoming photon is referred to as fluorescent radiation. Fluorescence, in general, is a process in which some of the energy of a photon is used to create a second photon of less energy. This process sometimes converts X-rays into light photons. Whether the fluorescent radiation is in the form of light or X-rays depends on the binding energy levels in the absorbing material.

2.2.2 Compton scattering

The Compton interaction is a purely kinematic collision between the incident gamma photon and an electron in the crystal that is either free or loosely bound as shown in Figure 2.1. The incident gamma ray has energy $E = h\nu$ that is shared between the Compton scattered photon and the recoiling electron. The photon will be scattered at a lower energy $h\nu'$ while the recoil electron will have energy of T_{e^-}.

Since the total energy is conserved in the interaction, one can write:

$$h\nu = h\nu' + T_{e^-} \tag{2.3}$$

where T_{e^-} is the kinetic energy of the ejected electron.

Since the linear momentum is also conserved in this interaction, then from the conservation of momentum along the x direction, and along the y direction, respectively, we get

In x-direction: $$\frac{h\nu}{c} = \frac{h\nu'}{c}\cos\theta + P\cos\phi \tag{2.4}$$

In y-direction: $$0 = \frac{h\nu'}{c}\sin\theta - P\sin\phi \tag{2.5}$$

where P is the linear momentum of the recoil electron.

But relativistically

$$Pc = \sqrt{T(T + 2m_o c^2)} \tag{2.6}$$

where m_o is the electron rest mass.

Hence, the energy of the scattered photon is given by

$$h\nu' = \frac{m_o c^2}{1 - \cos\theta + \left(\frac{1}{\alpha}\right)} \qquad \text{Where} \qquad \alpha = \frac{h\nu}{m_o c^2}$$

$$h\nu' = \frac{h\nu}{1 + \frac{h\nu}{m_o c^2}(1 - \cos\theta))}$$

$$E_\gamma' = \frac{E_\gamma}{1 + \frac{E_\gamma}{m_o c^2}(1 - \cos\theta))} \tag{2.7}$$

For a backscattered photon, i.e. $\theta = 180°$,

$$E_\gamma^{180°} = \frac{E_\gamma}{1 + \frac{2E_\gamma}{m_o c^2}} \tag{2.8}$$

and for $\alpha >> 1$, the energy of the backscattered photon approaches $(m_o c^2)/2$.

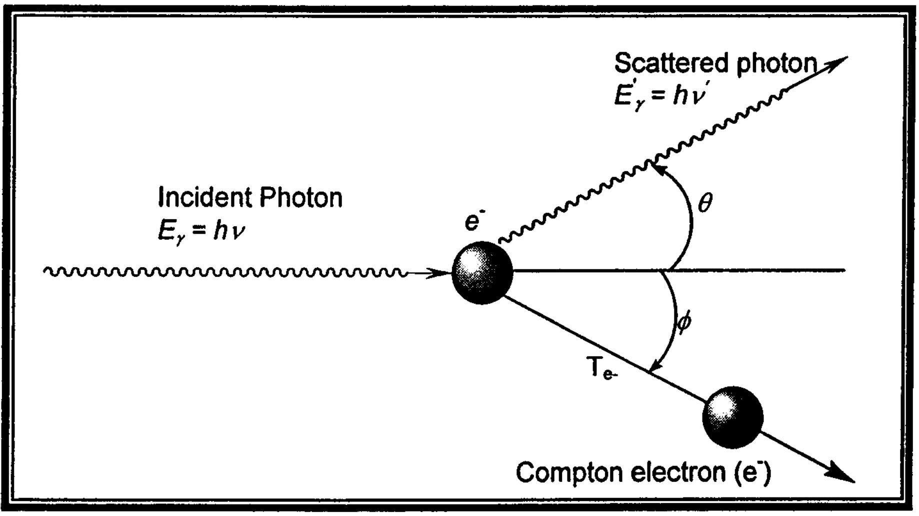

Figure 2.1 *Schematic diagrams showing a Compton scattering interaction. ν is the frequency of the incident photon, ν' is the frequency of the scattered photon and h is the Plank's constant.*

2.2.3 Pair production

When the photon energy exceeds 1.02 MeV (m_oc^2), annihilation of the photon occurs with the appearance of electron – positron pair in its place. The electron – positron pair has a total kinetic energy equal to the energy of the vanished photon:

$$E - 2m_oc^2 = T_{e-} + T_{e+} \tag{2.9}$$

where T_{e-} and T_{e+} are the kinetic energies of the electron and positron respectively. This process will only take place in the field of the nucleus and takes over as the dominant process as the photon energy increases.

2.2.4 Rayleigh (coherent) scattering

The Compton scattering process is an inelastic (incoherent) interaction where the scattered photon suffers deviation from its original direction, and carries a lower energy than the incident one. The Rayleigh scattering process, on the other hand, is an elastic (coherent) interaction where the incident photon does not lose any energy, but suffers deviation of small angles from its original direction so that no atomic excitation or ionization occurs to the atom. The Rayleigh scattering cross section, (White, 1950), of great importance at small photon energies, but it diminishes at higher energies due to the increased dominance of the inelastic process. The differential elastic cross section is given by:

$$\frac{d\sigma_R}{d\Omega} = \frac{d\sigma_{Th}}{d\Omega} F^2(q) \tag{2.10}$$

where the first term refers to Thomson cross section and the second term is the form factor scatter function.

Elastic scatter is predominant at small angles and in the diagnostic energy range or low momentum transfers that are single coherent scatter is much more intense than single Compton scatter. Within this region, single inelastic scatter is suppressed due to electron binding effects. Nevertheless, this is in conflict with the fact that the total inelastic cross-section is greater than the total elastic scatter cross-section (about 10 %). For example, the partial interaction cross-sections for oxygen over the diagnostic energy region (0-100 keV) shows photon attenuation is dominated by photoelectric absorption and incoherent (Compton) scatter and at no point is elastic scatter the major influence. This conflict is resolved by observing the differential cross-sections for scatter in the momentum range below 0.5 A^{-1} (corresponding to 10° at 70 keV) where coherent scatter is the dominant mechanism for photon scattering. By comparing both the coherent form factor function and the incoherent scattering function below the momentum transfer value stated above, it can be said that the coherent scatter is confined to a narrow forward scattering peak and the Compton scatter vanishes as the momentum transfer approaches zero due the incoherent scattering function.

2.3 X-ray absorption and scattering processes

Recall that photons are individual units of energy. Figure 2.2 illustrates the three possible fates of the individual photons when a beam of X-rays travels through matter. They may be:

(a) *Transmitted*: pass through unaffected, as primary or direct radiation.

(b) *Absorbed*: transferring to the matter all of their energy or some of it.

(c) *Scattered*: diverted in a new direction, with or without loss of energy, and so may leave the beam as scattered or secondary radiation.

X-ray absorption and scattering processes are stochastic processes, governed by the statistical laws of chance. It is impossible to predict which of the individual photons in a beam will be transmitted by 1 mm of the material, but it is possible to be quite precise about the fraction of them that will be, on account of the large numbers of photons it contains.

The interaction, either photoelectric or Compton, remove some of the photons from the beam in a process known as attenuation. Attenuation refers to the fact that there are fewer photons in the emerging beam than in the beam entering the material, which are caused by absorption and scattering effect when photons pass through the material.

Two general rules are:

(a) Photoelectric interactions occur most frequently when the electron binding energy is slightly less than the photon energy.

(b) Compton interactions occur most frequently with electrons with relatively low binding energy.

X-rays are not absorbed equally well by all material; if they were, they would not be very useful in diagnosis. Heavy elements such as calcium are much better absorbers of X-rays than light elements such as carbon, oxygen, and hydrogen, and as a result, structures containing heavy elements, like the bones, stand out clearly.

The soft tissues – fat, muscles, and tumors – all absorb about equally well and are thus difficult to distinguish from each other on an X-ray image. Of course, air is a poor absorber of X-rays.

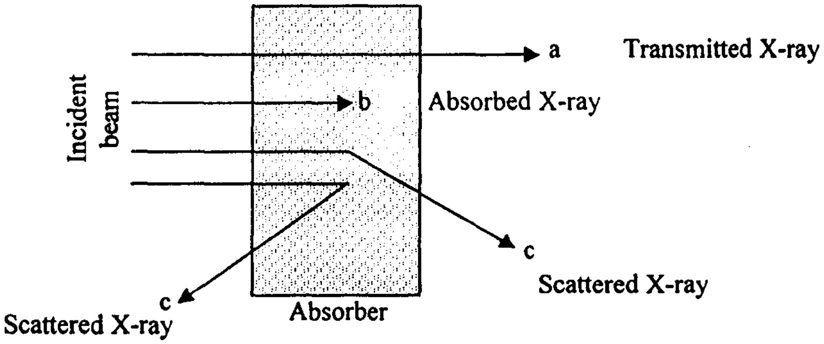

Figure 2.2 *Interaction of X-rays with matter.*

2.3.1 Photoelectric rates

The probability for photoelectric interaction to occur depends on how well the photon energies and electron binding energies match. This can be considered from two perspectives.

The more tightly the electron is bound to the atom and the nearer the photon energy is to its binding energy, the more likely photoelectric interaction is to happen. And so the probability that photoelectric interaction will occur decreases markedly as the photon energy of the radiation increases, being inversely proportional to the cube of the photon energy E. It increases markedly as the atomic number of the material increases, being proportional to the cube of the atomic number Z. In general, the conditions that increase the probability of photoelectric interactions are low photon energies and high atomic number materials.

2.3.2 Compton rates

Compton interactions can occur with the loosely bound electrons. The characteristic of the material that affects the probability of Compton interactions is the number of available electrons. Since the concentration of electrons in a given volume is proportional to the density of the materials, the probability of Compton interactions is proportional only to the physical density and not to the atomic number, as in the case of photoelectric interactions. In these materials with more electrons per gram, the probability of Compton interactions is enhanced. Although the chances of Compton interactions decrease slightly with photon energy, the change is not as rapid as for photoelectric interactions, which are inversely related to the cube of the photon energy.

2.3.3 Direction of scatter

It is possible for photons to scatter in any direction. The direction in which an individual photon will scatter is purely a matter of chance. There is no way in which the angle of scatter for a specific photon can be predicted. However, there are certain directions that are more probable and that will occur with a greater frequency than others. The factor that can alter the overall scatter direction pattern is the energy of the original photon. In diagnostic examinations, the most significant scatter will be in the forward direction. This will be an angle of scatter of only of few degrees. However, especially at the lower end of the energy spectrum, there is a significant amount of scatter in the reverse direction. Increasing primary photon energy causes a general shift of scatter to the forward direction.

2.4 Competitive interactions

As photons pass through matter, they can engage in either photoelectric or Compton interactions with the material electrons. The combination of the two types of interactions produces the overall attenuation of the X-ray beam. The factors that determine which of the two interactions are most likely to occur depends on the type of material that are attenuated and the photon energy.

The photoelectric interaction is proportional to Z^3/E^3, and is particularly high when the photon energy is just greater than the kinetic energy, E_k. The Compton interaction is independent of Z and little affected by E. Accordingly, photoelectric interaction is more important than the Compton process with high-Z materials as well as with relatively low-energy photons. Conversely, the Compton process is more important than photoelectric interaction with low-Z materials as well as with high-energy photons.

CHAPTER 3

PHOTON TRANSMISSION MEASUREMENTS USING X-RAY FLUORESCENT (XRF) SOURCES

3.1 Introduction

Mammographic procedures usually involve photons with energies less than 40 keV. To study the mass attenuation coefficient of the samples in this energy range we need a beam of radiation having discrete energies. Since an X-ray machine produces a broad continuous spectrum, it is not suitable for this study. What can be done is by putting a pure elemental absorber in the beam to produce a characteristic fluorescent X-ray (XRF). By changing the absorber element, a beam of monoenergetic photons at different energies can be gotten. In this stage the most suitable absorber for different photon energies will be determined.

3.2 X-ray source

3.2.1 X-ray tube specifications

Photon sources can be divided into eight categories: radioisotopes, natural or artificial which is either produced by accelerators or nuclear reactors, X-ray generators, electron synchrotrons, storage rings, positron annihilation, in beam neutron capture γ-rays, bremsstrahlung radiation from electron accelerators with filtering, and certain nuclear reactor fission products.

These photon sources produce either γ-ray or X-ray radiation, some of which are monoenergetic and others polyenergetic. The latter is connected either with